nature communications

Article

https://doi.org/10.1038/s41467-024-52094-y

Time Lens Photon Doppler Velocimetry (TL-PDV) for extreme measurements

Received: 7 June 2023

Accepted: 26 August 2024

Published online: 04 September 2024

Check for updates

Velat Kilic[1,2], Christopher S. DiMarco[2,3], Jacob M. Diamond[2,4], Pinghan Chu[5], K. T. Ramesh[2,4], Zhehui Wang[5] ✉ & Mark A. Foster[1,2] ✉

Capturing extreme surface velocities with >50 km/s dynamic range, which arise in shock physics such as inertial confinement fusion (ICF), is beyond the reach of conventional photon Doppler velocimetry (PDV) systems due to the need for extremely large electrical bandwidth under such conditions. The recent ignition in ICF calls for new velocimetry that can measure velocities exceeding 100 km/s. Time lens PDV (TL-PDV) is a solution where the high frequency beat signal from a conventional PDV system is periodically temporally magnified in the optical domain using a time lens. Here we experimentally demonstrate TL-PDV for the first time, validate the performance over a 74 km/s velocity range with high accuracy using a temporal magnification factor of 7.6, and verify excellent agreement with conventional PDV for laser driven micro-flyer experiments. TL-PDV currently provides the largest velocity dynamic range among PDV systems and is scalable to even higher velocities, which makes it an ideal candidate for material characterization under the most extreme conditions such as optimizing fuel efficiency in ICF experiments.

Photon Doppler velocimetry (PDV) has become an indispensable tool in measuring velocities that arise from shock physics such as laser driven micro-flyer studies[1–3], dynamic compression[4], and explosive detonation testing[5–7], due to its use of robust telecommunications optoelectronics such as low loss fiber optic components, narrow linewidth lasers, amplifiers and high speed detectors[8]. In its simplest form, conventional PDV systems transmit narrow linewidth laser light onto a target and collect the back reflected light. The moving target causes the reflected light to be Doppler shifted, which is then combined with a reference laser yielding a measurable beat frequency. At 1550 nm, every 1 km/s of target velocity leads to roughly 1.3 GHz of shift in the beat frequency. This scaling makes conventional PDV systems suitable for approximately 10 km/s velocity range given the bandwidth limitations of conventional digitizers.

Many variations on conventional PDV have been proposed that make use of frequency shifting, local oscillators with different wavelengths and the leapfrog PDV to increase the velocity dynamic range[8,9]. However, even with the PDV modifications above, the extreme velocities that arise from inertial confinement fusion (ICF) and other extreme experiments are often beyond the reach of PDV systems. ICF promises a sustainable energy source with great economic benefits if successful and ignition as recently announced[10] is a significant milestone in this direction. However, achieving sustainable fusion energy requires many optimization steps and diagnostics at extreme temperature, pressure and velocities (eg. 390 km/s reported in ref. 10). This creates an unmet need for accurate velocity characterization which is necessary for increasing efficiency. For example, an ideal ICF implosion requires isentropic compression of the fuel which is approximated by precise timing of a series of weak shocks designed to achieve quasi-isentropic compression[11]. Furthermore, magnetized target fusion (MTF) parameter space studies suggest velocities in the 100 km/s range is needed for ignition[12]. VISAR (velocity interferometry system for any reflector) has been the only option for extreme velocity diagnostics for these tasks[13], however it is an intensity based measurement which is susceptible to noise and often requires complicated and alignment sensitive free-space optical setups and streak cameras.

[1]Electrical and Computer Engineering, Johns Hopkins University, Baltimore, MD, USA. [2]Hopkins Extreme Materials Institute, Johns Hopkins University, Baltimore, MD, USA. [3]Sindri Materials Corp., West Chester, PA, USA. [4]Mechanical Engineering, Johns Hopkins University, Baltimore, MA, USA. [5]Los Alamos National Laboratory, Los Alamos, NM, USA. ✉e-mail: zwang@lanl.gov; mark.foster@jhu.edu

Further, VISAR systems struggle to measure multiple simultaneous surface velocities, are not compatible with the various multiplexing schemes employed by PDV systems and have very limited record lengths. In contrast, the popularity of PDV in shock physics has been attributed to its 'operational simplicity'[8], robustness to abrupt changes in surface reflectivity[14], the possibility of multiplexing schemes without commensurate increase in hardware complexity[15] and large record lengths. Furthermore, operating at 1550 nm provides the ability to amplify the return signal by many orders of magnitude with low noise figure due to low noise EDFAs (Erbium doped fiber amplifier).

The main limitation of conventional PDV systems is their limited velocity dynamic range resulting from the large electrical bandwidth requirements (e.g roughly 130 GHz bandwidth is required for 100 km/s). Several approaches have been investigated to overcome this limitation. As one highly relevant example, time stretch PDV (TS-PDV) has been proposed to overcome the bandwidth limitation through time-to-wavelength mapping and subsequent dispersion to "slow down" high frequency beat signals in the optical domain and in doing so, has brought PDV into the ICF range for the first time[16]. However, TS-PDV requires the PDV probe to illuminate the target with a wide-bandwidth chirped optical laser pulse, it suffers from the limitations associated with limited record length, non-uniform wavelength dependent amplification, and presents a complex experiment setup necessitating precise timing between the recording time window and experiment. Furthermore, as the time stretch[17] approach operates in the far-field dispersive regime, it requires the optical bandwidth to vastly exceed the PDV signal bandwidth and thus is highly bandwidth inefficient in the optical domain, which limits the achievable degree of stretching (or magnification), the maximum velocity that can be measured, as well as the ability to further wavelength multiplex PDV measurements. Time lens systems are preferable as they are significantly more bandwidth efficient[18], particularly for large time-bandwidth product PDV signals, which in turn allows for operation over larger velocity dynamic ranges.

Time lens PDV (TL-PDV) was recently proposed as an alternative method which temporally magnifies the beat signals using concepts from temporal imaging to create a time magnification system[17,19,20] as shown in Fig. 1. Four-wave mixing (FWM) in highly nonlinear fiber and

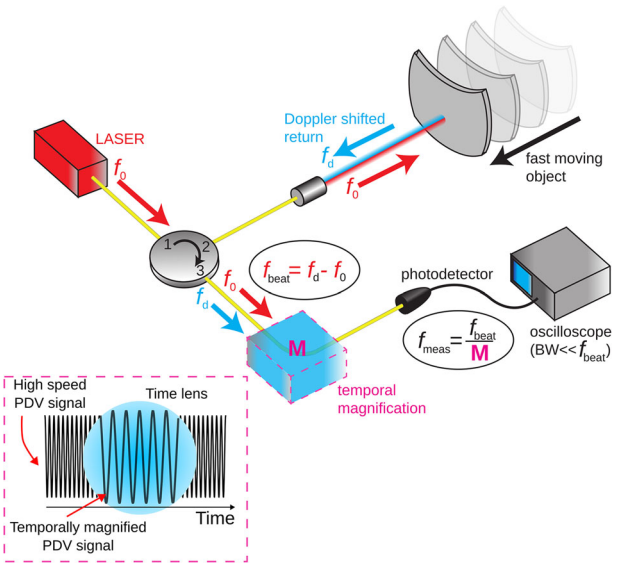

Fig. 1 | Conceptual drawing of a conventional PDV system modified by a time lens to enable measurements with high velocity dynamic range. A moving target is illuminated with CW laser light. Back-reflection is Doppler shifted due to the target motion. Both the reference and the Doppler shifted light is sent to a time lens for temporal magnification and subsequent detection.

appropriate amounts of dispersion in the pump, signal and idler arms are used to implement the time-lens and to create a temporal magnifier as shown in Fig. 2a. Here we experimentally demonstrate TL-PDV for the first time and show that a 74 km/s velocity range can be detected using only 12.5 GHz electrical bandwidth with a temporal magnification of 7.6. We also test the TL-PDV system on a laser-driven micro-flyer experiment in the low velocity range of the system (roughly 1 km/s) and show excellent agreement with a conventional PDV system. Our system enables measurements up to 74 km/s, which is currently the largest velocity dynamic range demonstrated among PDV systems. TS-PDV has been demonstrated up to only 44 km/s and leapfrog PDV[9] has been demonstrated up to 48 km/s, both with substantially larger electrical bandwidth than our demonstration here. Relative to TS-PDV, TL-PDV is experimentally simpler, makes better use of the optical bandwidth[18,21–23], and allows for a conventional narrow band continuous-wave (CW) PDV probe. Furthermore, scaling to higher magnification factors in TL-PDV is straightforward as switching between different magnification factors requires minimal changes to an existing time lens system. To this end, very high magnification factors are possible with related time lens systems such as the 103x[24], 158x[25] and 520x[26] demonstrated in the literature.

Results

Time Lens Design, Characterization and Calibration

To experimentally realize TL-PDV, we designed and implemented a time lens PDV system with 7.6x temporal magnification as shown in Fig 2b. To create the time lens pump, an optical filter in the 1547.47-1552.77 nm band is used to filter the broad band light from a 100 MHz mode locked laser (MLL) which yields a 5.3 nm pump bandwidth. Prior to the dispersion module, the pulse repetition rate is increased to 200 MHz via temporal multiplexing. After going through the dispersion module (201 ps/nm), the pulse width becomes roughly 1 ns. After amplification with a low power EDFA (Erbium doped fiber amplifier) and filtering to reduce noise from the ASE (amplified spontaneous emission), the pulses are further amplified with a high power EDFA (550 mW) to generate enough power for the FWM process. The signal arm has 6.73 km single mode fiber (SMF) which yields 114 ps/nm dispersion. The signal arm has a narrow band-pass filter (BPF) centered at 1541.35 to reduce ASE from the 150 mW EDFA. A matched (1547.47-1552.77 nm) WDM (wavelength division multiplexer) is used to combine the pump and the signal which reduces the ASE at the output of the 550 mW pump EDFA.

The idler is generated inside the 100m HNLF (highly nonlinear fiber) through FWM as shown in Fig. 2b. shows the spectra right after the HNLF where the idler appears at 1559 nm with 10.7 nm bandwidth. The idler arm also has a dispersion module, which is designed to compensate 50 km SMF and has a group delay dispersion (GDD) of -853 ps/nm. GDD in the signal, idler and the pump arms satisfy the imaging equation[19,27]

$$\frac{1}{D_s} + \frac{1}{D_i} = \frac{2}{D_p} \quad (1)$$

and leads to a magnification factor of 7.6. A small amount of pump light remains in the idler arm which is filtered out using a programmable filter (PF). Unfortunately, the PF has a relatively large insertion loss (5 dB), which reduces the sensitivity in our experiment but this can be avoided by using custom optical filters. The idler is then detected using an InGaAs detector with 15 GHz bandwidth and digitized using an oscilloscope with 12.5 GHz bandwidth.

In order to calibrate the time lens, we emulate Doppler shifts from high velocity targets using a tunable CW laser. In this experiment, the local oscillator is kept at 1541.47 nm while the other laser is scanned in the range 1540.70-1541.43 nm and its power is set to -15 dBm in order to emulate a typical low return signals from a target. The lasers are not

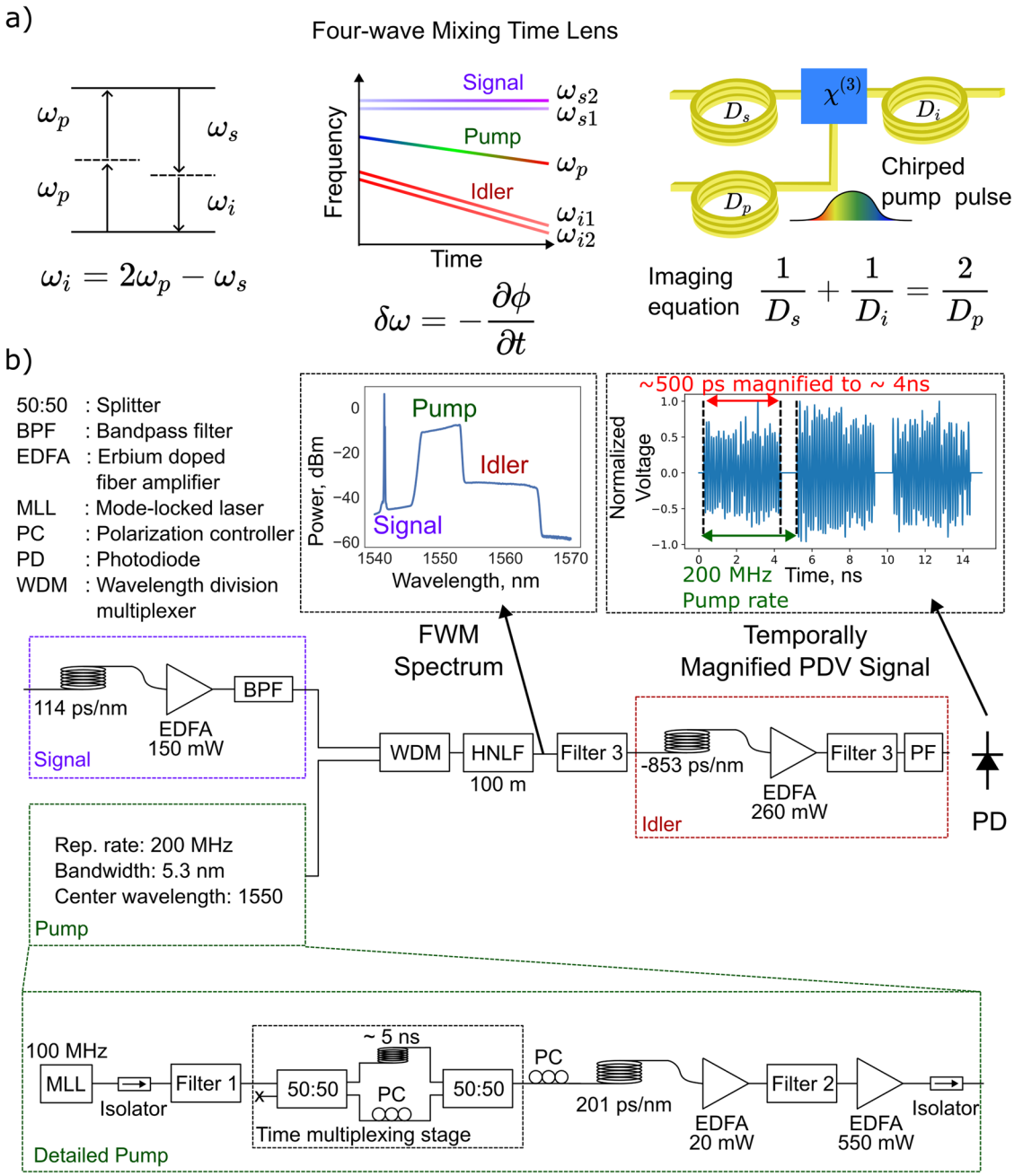

Fig. 2 | TLPDV experimental schematic. a Simplified four-wave mixing based time-lens diagram. Two pump photons are annihilated to create a signal and an idler photon which is stimulated by the signal photon. Interaction between a chirped pump pulse and a CW signal results in a chirped idler which has the phase and amplitude information from signal and a linear chirp from the pump. A local oscillator is combined with the PDV laser prior to the time lens and therefore creates its own chirped idler. Linear chirp implies quadratic temporal phase which is analogous to quadratic spatial phase for a free-space lens. Similar to the spatial imaging equation, a temporal imaging equation can be written which depends on the pump, signal and the idler dispersions. **b** Experimental diagram for the time lens is shown with 3 arms: the pump, the signal and the idler. The return signal from the PDV enters the time lens through the signal arm. Pump arm starts with a broad band mode locked laser which is filtered, chirped and amplified. Pump and the signal are combined and sent to a highly nonlinear fiber (HNLF). The inset shows the measured spectra at the output of the HNLF. Idler is filtered out, chirped and amplified. A programmable filter is used at the end to filter out any pump leakage. The inset shows the idler after detection, digitization, gain equalization and normalization.

locked together, but their relative phase drifts over a time period much longer than the experiment duration and therefore the beat frequency remains constant during this test. Figure 3 shows example pulses where the larger wavelength difference leads to higher frequencies. The FFT amplitude plots demonstrate the signal processing pipeline where the frequency at the peak maximum is used to estimate the beat frequency per pulse. Temporal magnification calibration plot is then generated from the average of these measured frequencies using 199 pulses. The orange band shows $\pm 2\sigma$ around the average which corresponds to a 95% confidence interval assuming normal distribution where σ is the standard deviation. Blue line shows the design magnification factor which matches the experiment well.

In order to better characterize the input power sensitivity, we keep the local oscillator at 1541.47 nm and set the input wavelength to 1541.00. The input power is then varied in the range −3 dBm to −21 dBm in steps of 3 dB. Figure 4 shows example measurements and the corresponding FFT amplitudes. The frequencies at the peak amplitudes are extracted and the standard deviation is calculated from 199

https://doi.org/10.1038/s41467-024-52094-y

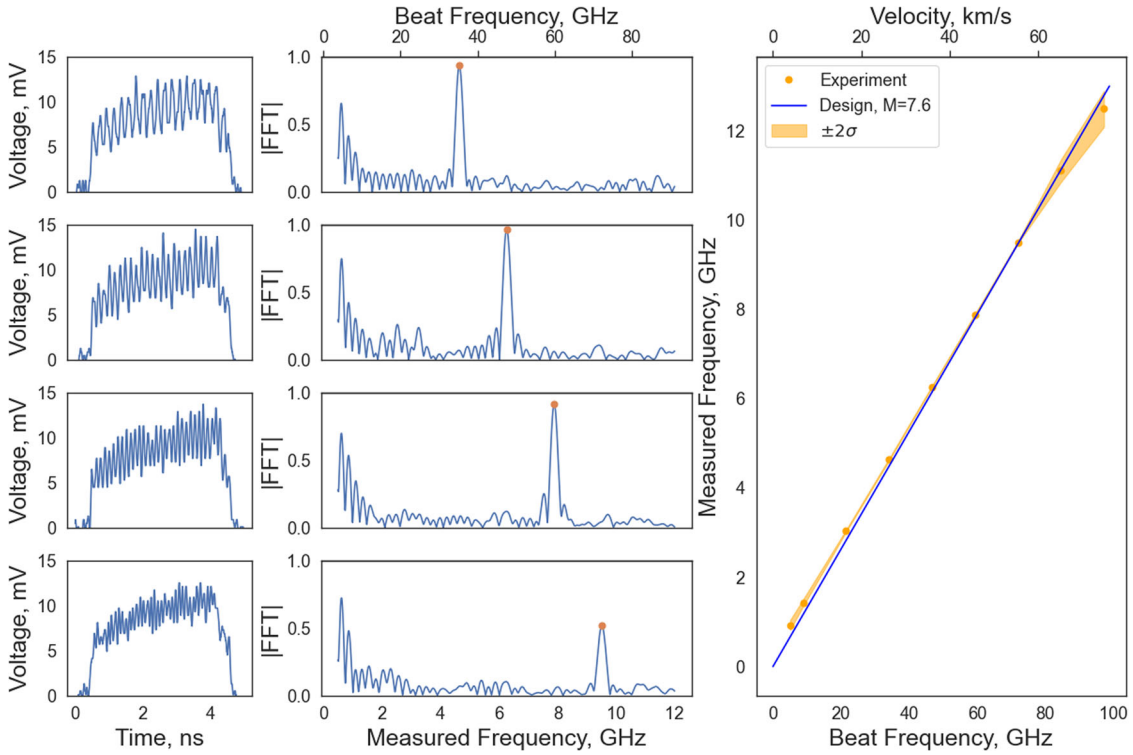

Fig. 3 | Temporal magnification measurement. Two CW lasers are combined to emulate large Doppler shifts and to calibrate the time lens. One of the lasers is set to 1541.47 nm and the other one is varied in the range 1540.70–1541.43 nm with a low −15dBm power to emulate weak return signals from a target. The first two columns show the idler time trace and the corresponding Fourier transform amplitudes for input wavelengths of 1541.20 nm, 1541.10 nm, 1541.00 nm and 1540.90 nm. The measured frequencies can be extracted from the peak position of the FFT amplitudes. The right panel shows the measured frequencies from these FFT maxima and the set frequencies calculated from the wavelength difference are plotted and show excellent agreement between the design and the measured temporal magnification. The yellow band shows $\pm 2\sigma$ estimated from 199 pulses where σ is the standard deviation.

pulses. This standard deviation is converted to a fractional velocity uncertainty and plotted against the input power. As shown in Fig. 4, input power sensitivities as low as −21 dBm are possible with fractional velocity uncertainties of better than 3×10^{-3}. Notably, we use a 50:50 coupler to combine the local oscillator and the return signal with the intention to time multiplex another time lens for future work which would increase sampling rate to 400 MHz.

Laser Driven Micro-flyer (LDMF) experiments with TL-PDV

To validate that TL-PDV can measure surface velocities under real-world operating conditions, we tested the TL-PDV system on a laser-driven flyer experiment[28,29] as shown in Fig. 5a shows the PDV set-up where the CW lasers are used in a heterodyne set-up to measure the surface velocity of the flyer. Output of the single mode fiber (SMF) is mapped onto the target surface using a 4f system (f_1 = 2.54cm and f_2 = 20 cm). The sample sits inside a vacuum chamber as shown in Fig. 5b and is surrounded by multiple diagnostic systems: PDV, front and back camera systems for alignment and a high-speed camera to image the flyer. Figure 5c shows a cartoon diagram of the flyer stack where a YAG laser illuminates the back side and boils off the epoxy laser which rapidly expands and propels the aluminum (Al) disc. Figure 5d shows the Al disc in flight for a duration much longer than the PDV measurement window. Most physically interesting phenomena occurs shortly after the flyer launch. Note, even though these flyers move incredibly fast (≈1 km/s), their velocities are still orders of magnitude smaller than velocities that arise from ICF experiments. Therefore, in this demonstration, the TL-PDV system is capturing dynamics at the extreme low end of its velocity dynamic range. Figure 6a shows a raw TL-PDV trace from a flyer experiment cropped to ± 200ns around the launch. Zooming in time as shown in Fig. 6b shows periodically and temporally magnified windows before and after he launch. Figure 6c shows the FFT amplitudes for each time window. Zooming in, Fig. 6d shows a very small Doppler shift due to temporal magnification which corresponds to roughly 600 m/s measured using a TL-PDV system with 74 km/s velocity range.

In Fig. 7, we compare velocity traces from different LDMF experiments with the same flyer parameters (100 µm thick Al flyers with 1.55 mm thickness) to compare PDV and TL-PDV measurements. The top row shows conventional PDV spectrograms for flyers driven by a high energy YAG laser at two different pulse energies. Terminal velocities are between 600–800 m/s, which yields roughly 0.7 GHz to 1 GHz frequency shifts. In contrast, the TL-PDV system with 7.6 magnification factor yields 0.1 GHz to 0.13 GHz frequency shifts as shown in the bottom row. While these shifts are smaller than the Fourier width of the FFT given the 5-ns time window, the peak position of the FFT amplitude nevertheless gives a good estimate of the frequency shift[30] when signal-to-noise ratio is high. This is similar to the super-resolution techniques used in microscopy[31]. The bottom row of Fig. 7 shows TL-PDV velocity recordings for the laser driven flyers using this extraction approach. Excellent agreement is observed between the TL-PDV velocity recordings and those of the conventional PDV system for both launch laser pulse energies. Notably, due to experimental limitations, the TL-PDV and conventional PDV data are not collected on the exact same launch event and thus exact agreement between the displayed data is not expected.

Discussion

We experimentally demonstrate a TL-PDV system for the first time and show that it can be used to measure a large velocity range using lower bandwidth electronics and off-the-shelf fiber optic components. The current electrical bandwidth of 12.5 GHz and temporal magnification of 7.6 yields a velocity range of 74 km/s with less than 100 m/s

https://doi.org/10.1038/s41467-024-52094-y

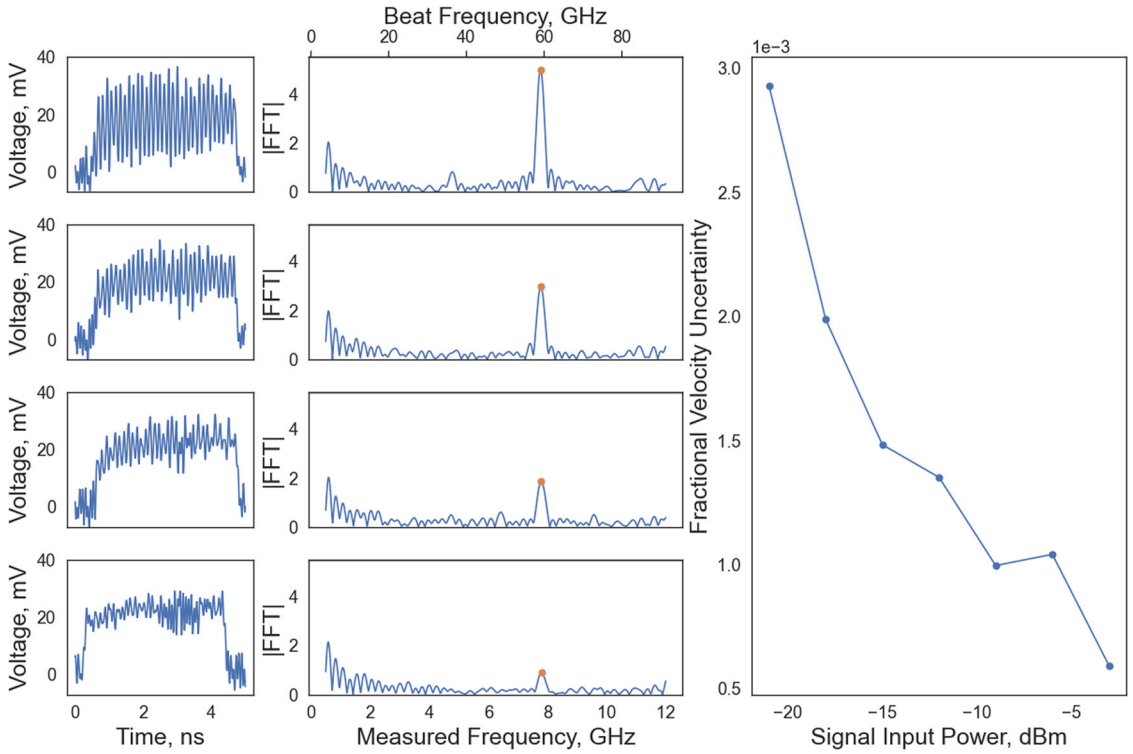

Fig. 4 | Power sensitivity measurement. In order to characterize the power sensitivity, we vary the input power from −21 dBm to −3 dBm in 3dB steps. The first two columns show the time traces as well as corresponding FFT amplitudes for input powers −3, −9, −15 and −21 dBm. In the right panel, 199 pulses are used to calculate the standard deviation for a given input which is then converted to a velocity uncertainty as a function of input power.

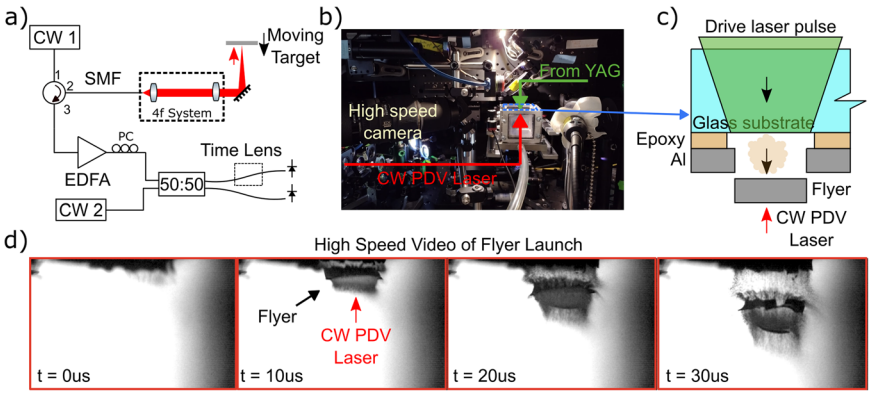

Fig. 5 | Laser-driven micro-flyer (LDMF) experiment. a Schematic for measuring LDMF velocities. Single mode fiber (SMF) is imaged on to the target surface using a 4f system. The return signal is amplified and combined with a local oscillator. TL-PDV is optionally inserted into the system to temporally magnify the PDV signal. **b** Experiment set-up picture. SMF is imaged onto the back surface of the flyer stack. A YAG laser is focused on the top surface. A high speed camera observes the experiment laterally. **c** A schematic of the flyer stack. Pulsed laser boils a thin epoxy laser and propels an aluminum disc. **d** High speed camera frames for an example shot.

uncertainty at low return signal powers. For a single TL-PDV channel, sensitivity can be further improved by a different coupler ratio, e.g., 99:1. Current set-up can sufficiently sample the velocity curves from the Z-machine[9]. However, sampling the velocities from the ICF experiment at the National Ignition Facility (NIF)[10] requires eliminating the gaps in the observation window which arise from a measurement window-temporal magnification trade-off. This problem can be addressed using time multiplexing schemes as shown in Fig 8 where a 1μs window of a PDV signal is carved out and sent through 3 multiplexing stages resulting in the generation of 8 replicas of the 1μs PDV signal. This stage can be inserted into the signal arm prior to our time lens system to enable continuous measurement over a 1μs time window with a temporal magnification of up to 8× . Continuous sampling is enabled by slightly shifting the temporal pump alignment to the PDV signal by the 500 ps pump window on each replica allowing capture of the dynamics in the gaps between pump pulses. In general, full sampling of a given time window using a temporal magnification of M requires $\log_2(M)$ time multiplexing stages which scales well to large M.

In contrast to TS-PDV which requires precise timing of the measurement window, the free-running nature of our TL-PDV implementation enables very long record times which adds to its operational simplicity. We believe the TL-PDV system will pave the way for better velocity measurements and equation of state (EOS) characterization in

https://doi.org/10.1038/s41467-024-52094-y

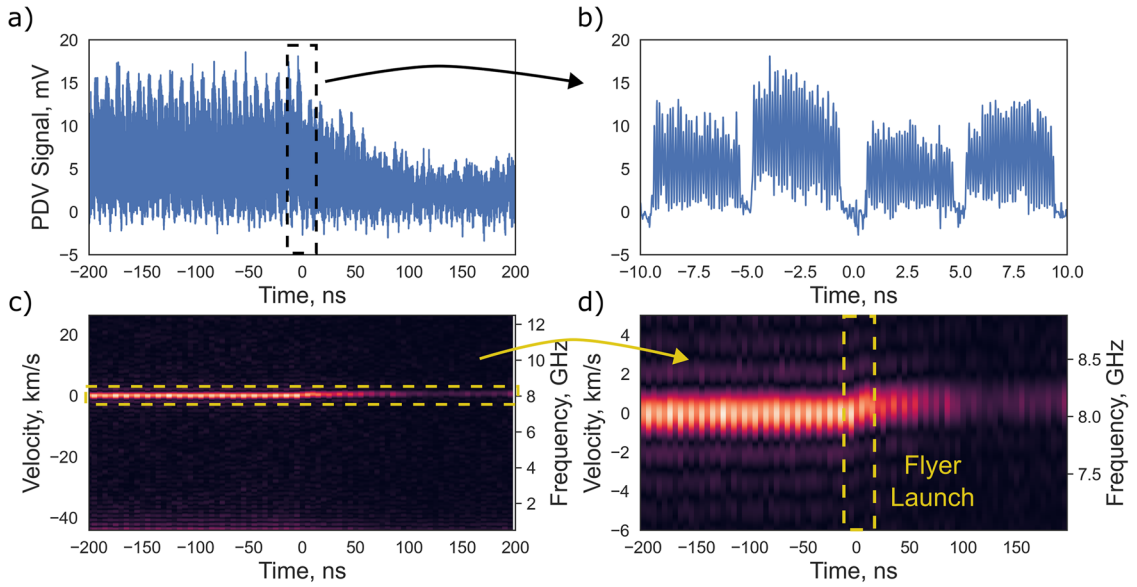

Fig. 6 | TL-PDV signal from an LDMF experiment. a TL-PDV trace from an 100 µm thick flyer driven by a 1J YAG laser pulse. **b** Zoomed in TL-PDV trace shows periodically and temporally magnified beat frequency. **c** Corresponding short-time FFT spectrogram shows the entire 74 *km/s* velocity range. **d** Zoomed in spectrogram shows the small frequency shift due the flyer movement.

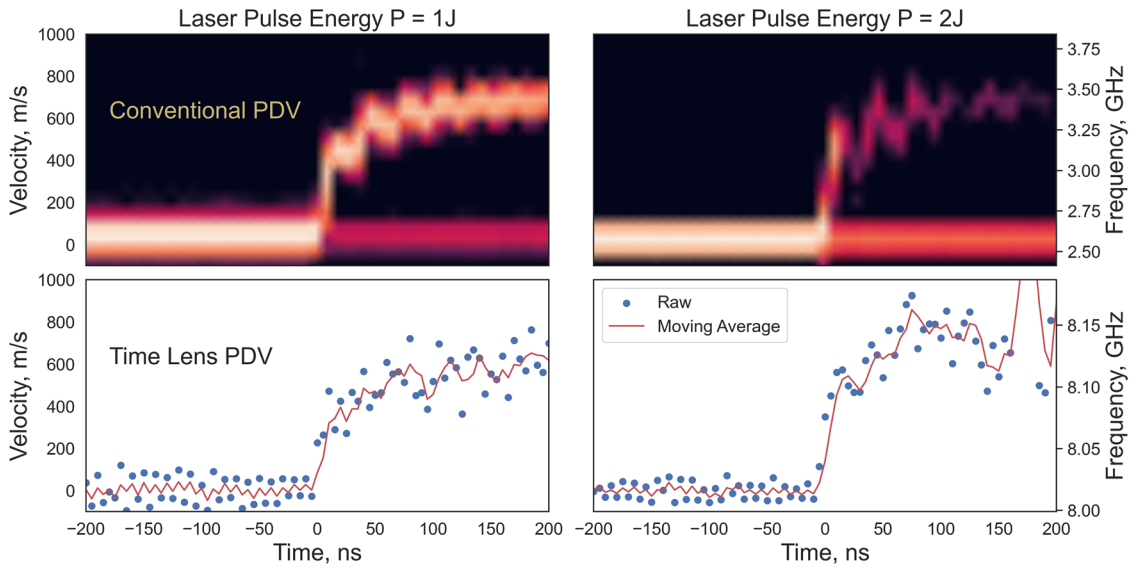

Fig. 7 | TL-PDV and conventional PDV comparison for 100µm thick Al flyers driven by two different pulse energies. All shots are from different flyers that have similar material composition and geometry. Red solid line shows the three-point moving average.

extreme environments, specifically those that arise in inertial confinement fusion. Achieving sustainable fusion energy will likely require many optimization steps which will be informed by diagnostics under extreme conditions. TL-PDV has the promise to improve velocity diagnostics and potentially lead to better fuel optimization.

Methods

TL-PDV experiments

Off-the-shelf fiber optic components are used for the TL-PDV setup. 100 MHz mode locked laser is the C-Fiber from Menlo Systems. OFS SLAM +200 and SMF-DK 50 are used for the 201 ps/nm and −853 ps/nm dispersion modules respectively. We spooled the 6.73 km SMF in house using a Unispooler machine. Waveshaper 1000A from Finisar is used for the programmable filter. EOT ET-3500F is the InGaAs detector and Tektronix DPO71254C is the oscilloscope used to record the PDV traces. Time lens design magnification is calculated using the frequency domain variables $\beta_2 L$ and the center wavelength of the idler which yields $\frac{(\beta_2 L)_i}{(\beta_2 L)_s} = \frac{1.0997 \times 10^{-21} s^2}{1.4419 \times 10^{-22} s^2} \approx 7.6$

Flyer preparation

The flyers used in this study are circular disks with a diameter of 1.5mm and a thickness of 100 µm. They are fabricated in 7 × 7 arrays using a glass-epoxy-metal layered structure. The glass component is a 50 × 50 × 0.625 mm boroscilicate plate from McMaster Carr (p/n B8476012), while the epoxy is a two-part mixture from Ellsworth (Henkel Loctite Ablestik 24). The flyers themselves are made from aluminum sheets from AluFoil, with the thickness corresponding to the flyer thickness. The glass and aluminum are cleaned using acetone and IPA, then epoxied together and held under a constant compression pressure for over 24 hours to cure. Finally, a Clark-MXR femtosecond laser is used

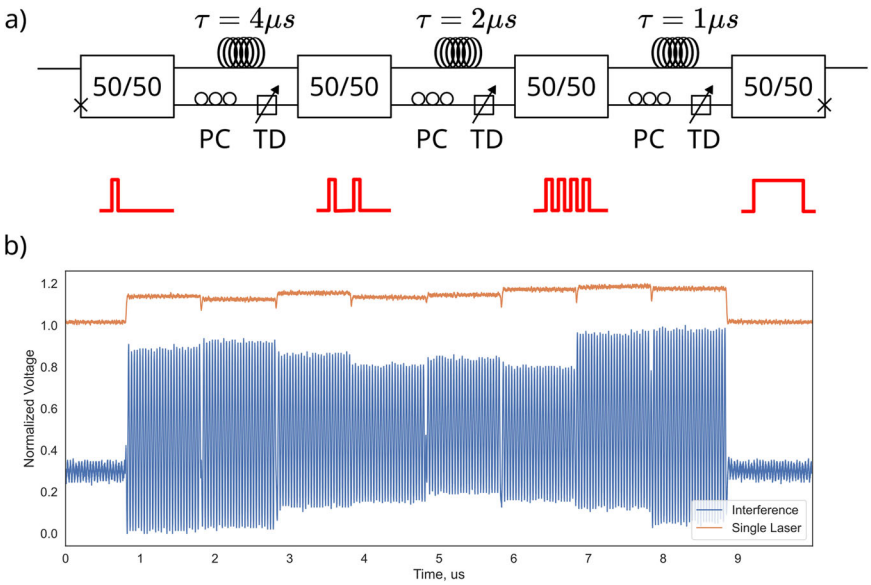

Fig. 8 | Signal arm temporal multiplexing. a Temporal multiplexing on the signal arm. A 1us pulse is carved out from the signal which is then split and delayed using coupler, polarization controllers (PC) and tunable delay (TD) lines. **b** Experimental measurement showing 8x time multiplexing. When tunable delays are set properly, a temporal multiplexing factor of $log_2(M)$ can enable continuous measurement window for a temporal magnification M.

to cut out a 7 × 7 array of flyers from the aluminum, through the entire thickness. The spacing between flyers is 6 mm, which is sufficient to ensure that adjacent launches do not interfere with one another.

Flyer launch experiment

The laser-driven micro-flyer experiment involves the use of a high-energy laser pulse to achieve high velocities for a small flyer. Specifically, a 1064-nm Nd:YAG laser with a 2.5 J energy, 10-Hz frequency, and 10-ns duration is used with a beam quality (M^2 value) of approximately 15 (Spectra Physics Quanta-Ray Pro-350). To optimize launch conditions, free-space optics are used to increase the pulse diameter to approximately 25 mm, lengthen the pulse temporally to 21 ns through an optical cavity, and shape it to a low variation top-hat spatial profile using a Silios Technologies diffractive optical element in conjunction with a 250 mm focusing lens. The focused beam is aligned through the laser-transparent glass side of a glass-epoxy-flyer composite and onto the epoxy, which is ablated by the laser, leading to the expansion of hot gases and the ejection and acceleration of the flyer. The diameter of the focused laser is 1.85 mm, determined by the effective focal length of the focusing lens. The laser fluence, which is the primary driver of the flyer velocity, can be adjusted by changing the laser energy through an attenuator comprising a half-wave plate and a polarizing beamsplitter. In addition to the TL-PDV diagnostic focused on the free-surface of the flyer to measure the normal flyer velocity, and a Shimadzu high-speed camera operating at 10,000,000 frames/second provides a side view of the flyer launch process.

Data availability

The PDV data generated in this study and the code used to process the data have been deposited in the Zenodo database[32].

References

1. Mallick, D. D. et al. Spall strength in alloyed magnesium: a compendium of research efforts from the cmede 10-year effort. *Mech. Mater.* **162**, 104065 (2021).
2. Weng, J. et al. A compact all-fiber displacement interferometer for measuring the foil velocity driven by laser. *Rev. Sci. Instrum.* **79**, 113101 (2008).
3. Li, F. & Dlott, D. D. High throughput tabletop shock techniques and measurements. *J. Appl. Phys.* **131**, 075901 (2022).
4. La Lone, B. et al. Simultaneous broadband laser ranging and photonic Doppler velocimetry for dynamic compression experiments. *Rev. Sci. Instrum.* **86**, 023112 (2015).
5. Yadav, H., Kamat, P. & Sundaram, S. Study of an explosive-driven metal plate. *Propellants Explos. Pyrotech.* **11**, 16–22 (1986).
6. Danielson, J. et al. Measurement of an explosively driven hemispherical shell using 96 points of optical velocimetry. In: *Journal of Physics: Conference Series*, vol. 500, p. 142008 (IOP Publishing, 2014).
7. Briggs, M.E., Hill, L.G., Hull, L.M., Shinas, M., Dolan, D. Applications and principles of photon-doppler velocimetry for explosive testing. In: *Proceedings of 14th International Detonation Symposium* (2010)
8. Dolan, D. Extreme measurements with photonic Doppler velocimetry (pdv). *Rev. Sci. Instrum.* **91**, 051501 (2020).
9. Dolan, D. et al. Tracking an imploding cylinder with photonic Doppler velocimetry. *Rev. Sci. Instrum.* **84**, 055102 (2013).
10. Abu-Shawareb, H. et al. Lawson criterion for ignition exceeded in an inertial fusion experiment. *Phys. Rev. Lett.* **129**, 075001 (2022).
11. Craxton, R. et al. Direct-drive inertial confinement fusion: a review. *Phys. Plasmas* **22**, 110501 (2015).
12. Lindemuth, I.R. The ignition design space of magnetized target fusion. *Phys. Plasmas* **22**, 122712 (2015).
13. Celliers, P.M., Millot, M. Imaging velocity interferometer system for any reflector (visar) diagnostics for high energy density sciences. *Rev. Sci. Instr.* **94**, 011101 (2023).
14. Jensen, B., Holtkamp, D., Rigg, P. & Dolan, D. Accuracy limits and window corrections for photon Doppler velocimetry. *J. Appl. Phys.* **101**, 013523 (2007).
15. Frayer, D.K., Fratanduono, D. Considerations for a pdv diagnostic capability on the national ignition facility. In: *Target Diagnostics Physics and Engineering for Inertial Confinement Fusion V*, vol. 9966, pp. 81–91 (2016). SPIE
16. Mance, J. et al. Time-stretched photonic Doppler velocimetry. *Opt. Express* **27**, 25022–25030 (2019).
17. Bennett, C.V., Kostinski, N.B. Fourier analysis by spectral transformation (Fast) Photonic Doppler Velocimetry (PDV) with signal fade mitigation. *Google Patents. US Patent* 10, 379, 223 (2019)

18. Salem, R., Foster, M. A. & Gaeta, A. L. Application of space–time duality to ultrahigh-speed optical signal processing. *Adv. Opt. Photonics* **5**, 274–317 (2013).
19. Chu, P., Kilic, V., Foster, M. A. & Wang, Z. Time-lens photon doppler velocimetry (tl-pdv). *Rev. Sci. Instrum.* **92**, 044703 (2021).
20. Crockett, B., Rowe, C., Azaña, J. Capturing ultra-broadband complex-fields of arbitrary duration using a real-time spectrogram. *APL Photonics* **8**, 066108 (2023).
21. Foster, M. A. et al. Silicon-chip-based ultrafast optical oscilloscope. *Nature* **456**, 81–84 (2008).
22. Bennett, C. V. & Kolner, B. H. Principles of parametric temporal imaging. i. system configurations. *IEEE J. Quantum Electron.* **36**, 430–437 (2000).
23. Bennett, C. V. & Kolner, B. H. Principles of parametric temporal imaging. ii. system performance. *IEEE J. Quantum Electron.* **36**, 649–655 (2000).
24. Bennett, C. & Kolner, B. Upconversion time microscope demonstrating 103 × magnification of femtosecond waveforms. Opt. Lett. 24, 783–785 (1999).
25. Joshi, C. et al. Picosecond-resolution single-photon time lens for temporal mode quantum processing. *Optica* **9**, 364–373 (2022).
26. Salem, R. et al. High-speed optical sampling using a silicon-chip temporal magnifier. *Opt. Express* **17**, 4324–4329 (2009).
27. Salem, R. et al. Optical time lens based on four-wave mixing on a silicon chip. *Opt. Lett.* **33**, 1047–1049 (2008).
28. Mallick, D. et al. Laser-driven flyers and nanosecond-resolved velocimetry for spall studies in thin metal foils. *Exp. Mech.* **59**, 611–628 (2019).
29. Mallick, D. et al. A simple dual-beam time-multiplexed photon Doppler velocimeter for pressure-shear plate impact experiments. *Exp. Mech.* **59**, 41–49 (2019).
30. Dolan, D. Accuracy and precision in photonic Doppler velocimetry. *Rev. Sci. Instrum.* **81**, 053905 (2010).
31. Mortensen, K. I., Churchman, L. S., Spudich, J. A. & Flyvbjerg, H. Optimized localization analysis for single-molecule tracking and super-resolution microscopy. *Nat. methods* **7**, 377–381 (2010).
32. Kilic, V., DiMarco, C., Diamond, J., Foster, M. Time Lens Photon Doppler Velocimetry (TL-PDV) for Extreme Measurements [Data Set]. https://doi.org/10.5281/zenodo.13117852

Acknowledgements

This work is supported in part by the Advanced Diagnostics program (C3) at LANL (V.K., P.C., Z.W., M.A.F.), in part by the NSF DMREF program (C.S.D, J.M.D, K.T.R.), and in part by the Department of the Defense, Defense Threat Reduction Agency under award HDTRA1-20-2-0001 (V.K., K.T.R, M.A.F.).

Author contributions

M.A.F. and V.K. designed the time lens and the calibration setup. V.K. built and calibrated the time lens. C.S.D. and J.D. prepared the LDMF samples. V.K., C.S.D. and J.D. performed the laser-driven flyer experiments. P.C., K.T.R., Z.W. and M.A.F. supervised the project. All authors contributed to project discussions and the writing of the manuscript.

Competing interests

The authors declare no competing interests.

Additional information

Supplementary information The online version contains supplementary material available at https://doi.org/10.1038/s41467-024-52094-y.

Correspondence and requests for materials should be addressed to Zhehui Wang or Mark A. Foster.

Peer review information *Nature Communications* thanks the anonymous reviewers for their contribution to the peer review of this work. A peer review file is available.